Modeling and Target Classification Using Multiple Reflections of Sonar

Wangheon Lee, Kukjin Yoon and Inso Kweon

Department of Electrical Engineering & Computer Science
Korea Advanced Institute of Science and Technology
373-1 Kuseong-dong, Yuseong-gu, Daejeon, Korea

{whlee, kjyoon }@rcv.kaist.ac.kr, iskweon@kaist.ac.kr

Abstract

This paper describes a sonic polygonal multiple reflection range sensor (SPMRS), which uses multiple reflection properties usually ignored in ultrasonic sensors as disturbances or noises. Targets such as a plane, corner, edge, or cylinder in indoor environments can easily be detected by the multiple reflection patterns obtained with a SPMRS system. Target classification and feature data extraction, such as distance and azimuth to the target, are computed simultaneously by considering the geometrical relationships between the detected targets, and finally the environment model is generated by refining the detected targets. In addition, the narrow field of view of a sonar range sensor is increased and the scanning time is reduced by active motion of the SPMRS stepping servomechanism.

Keywords:
Polygonal reflector, Multiple reflections, Ultrasonic sensor, Mobile robot

1 Introduction

A motive for using sonar for mobile robot navigation is its ease of use and low cost. Despite some successes with the use of time of flight (TOF) sonar in robotics, results have generally been disappointing because of diffraction and multiple reflections, which are inherent characteristics of sonar.

Because TOF patterns from a plane or corner have similar patterns when the transmitter is rotated by small increment, it is impossible to discriminate target types by using TOF information alone [1].

Map generation methods applying the KALMAN filter to TOF data obtained by rotating sonar were proposed and could reduce angular uncertainty by multiple returns, but it involves considerable scanning time [2] [3].

A target discrimination method requiring convolution integration between the source and the transfer function, which is derived from the relationship between the indoor target and the sonar source modeled as an envelope function [4], has been proposed. However, it is not possible to recognize the target in a complex environment where more than one target, such as a corner, plane or edge, is present.

To resolve these problems in conventional TOF-based methods, we propose a new recognition method that actively uses the multiple reflection properties of sonar.

We developed a sonic polygonal multiple reflection range sensor (SPMRS) system composed of seven polygonal reflectors to generate multiple reflections easily and to reduce scanning angle, which consumes most of the time in acquiring one frame of multiple reflection data.

The proposed SPMRS system also reduces the scanning angle to 30° rather than 360°, to collect multiple reflection information of the surrounding environment.

2 SPMRS System Modeling

2.1 Reflection patterns and SPMRS system modeling

Fig.1 shows the reflected waveforms for the corner and the plane by the TOF and the multiple reflection system, respectively, but it is not easy to discriminate the target type and azimuth for each target only by the TOF data.

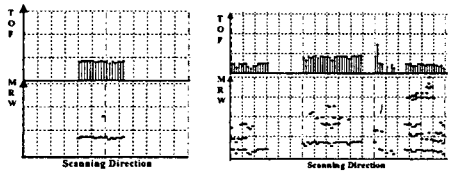

(a) plane target (b) corner target

Fig.1 Multiple reflection waveforms (**MRW**) and time of flight (**TOF**) waveforms in corner and plane target 100 cm apart from the reflector: the upper is TOF waveforms, and the lower is multiple reflection waveforms obtained by SPMRS, respectively.

And so in this paper, we take advantage of the multiple reflections usually ignored as noises or disturbances so as to recognize the target type, azimuth and distance, simultaneously, where we especially utilize triangular shapes including the target type and azimuth information made by the multiple reflection patterns along the scanning direction.

To begin with, the acoustic cone, defined as in Eq.(1) [1], is quantized so that the multiple reflection phenomena

could be easily explained as shown in Fig.2(b).

$$\theta_0 = \sin(\frac{0.16\lambda}{a}), \quad A(\theta) = A_{max} e^{-\frac{4\theta^2}{\theta_0^2}} \qquad (1)$$

where θ_0 is the acoustic cone, λ is the sound wavelength, a is the radius of the transducer and $A(\theta)$ is the sound intensity (Fig.2(a)).

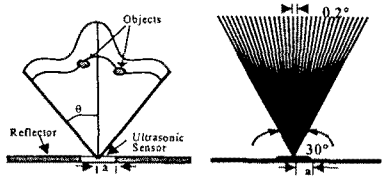

(a) F.O.V. of SPMRS (b) quantized sonar model
Fig.2 Field of view and quantized sonar model.

The viewing angle of the ultrasonic sensor is shown in Fig.2(a), where the θ is the angle within which the sensor can detect the object by transmitting its ultrasonic waveform and the a is the radius of the ultrasonic transducer [4].

In this research, by using this acoustic cone model quantized by equal increments of 0.2° (Fig.2(b)) and assuming the ultrasonic waves transmitted to the target directly, we can easily analyze the traveling path of the ultrasonic wave in the indoor environment.

Fig.3(a) shows the virtual reflection model [5] and also Fig.3(b) shows a simulated multiple reflection scanning model using quantized acoustic cone and virtual reflection between the reflector and plane target.

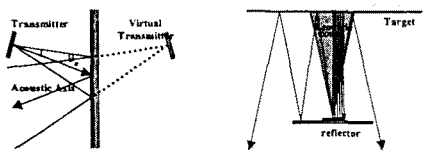

(a) (b)

Fig.3 Virtual reflection pattern and its simulation model: (a) virtual mirror model, (b) simulated multiple reflection scanning model using a quantized SONAR model.

If the scanning angle is greater than θ_0, the reflected wave misses the target and the multiple reflection phenomena are not observed. As experimental targets, we take four types of object (Fig.4) frequently encountered in indoor environments [1][2][6].

(a) plane (b) corner (c) edge (d) cylinder

Fig.4 Basic targets for the recognition test.

The multiple reflection scanning model can be easily explained by the same virtual mirror model [1][5] (Fig.3(a)).

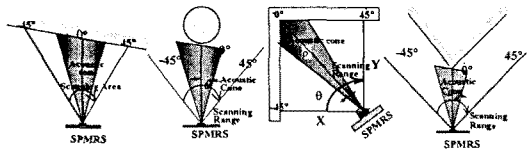

(a) plane (b) cylinder (c) corner (d) edge
Fig.6. The multiple reflection scanning model for indoor targets.

The diffracted reflection occurs at the edge target with a reflection surface smaller than the wavelength of the transmitted ultrasonic sound as shown in Fig.6 (d) and the diffracted waveforms propagate in all direction from the edge target, and so the multiple reflection does not generated in this edge target [1].

Based on these analyses, we attached the reflector purposely behind the ultrasonic transducer so that reflections can be easily generated between the indoor target and the ultrasonic sensor as shown in Fig.7 (a), and Fig.7(b) shows the multiple reflection pattern between one reflector and a plane target 100 cm apart from the reflector, where the SPMRS is fixed to face the plane directly.

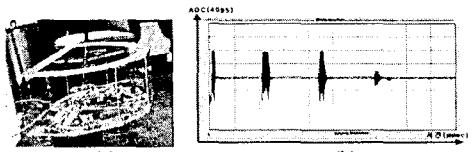

(a) (b)

Fig.7 Configuration of SPMRS: (a) external view of SPMRS, (b) multiple reflection patterns between a plane target and a reflector with the target directly facing the reflector.

We therefore consider that the waveform transmitted initially from the ultrasonic ranging unit plays the part of an ultrasonic source after reflection from the object.

Fig.8 shows simulated multiple reflection patterns for the scanning models shown in Fig.6. We define the step distance (**SD**) as the difference between the first step and the last step that shows any reflection continuously appearing along the rotation angle axis, and define the number of multiple reflections (**NMR**) as the maximum count(s) of multiple reflections between the reflector and the target, which is located at the center of SD, as shown in Fig.8.

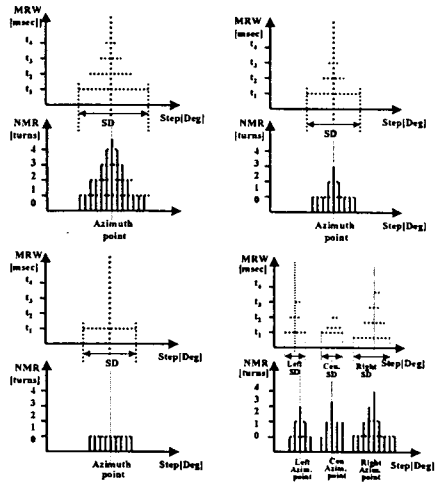

Fig.8 Simulated multiple reflection pattern and its notation for (a) plane target, (b) cylinder target with diameter 45 cm, (c) edge target and (d) corner target.

Fig.8 shows two kinds of geometrical multiple reflection shape (GMRS) along the scanning direction: a triangle and a rectangle.

Both the plane and the cylinder have only one triangular GMRS(1) with NMR for the plane target being larger than that for the cylinder. The corner target has three triangular GMRS(3). There is only one rectangular GMRS(1) for the edge target irrespective of the distance from the reflector.

2.2 Configuration of a seven polygonal reflection range sensor

2.2.1 Geometrical configuration

Seven reflectors are attached around the circumference of SPMRS in equal arcs of 30° (Fig.7(a)). The scanning operation is executed from reflector No.0 to reflector No.6 in a numbered sequence, and 2000 samples are taken every 10μs at each step.

We can obtain 420kByte of data in one frame of environment information through each of the 210 steps of the scanning operation.

Because the frame data include not only the environment information but also noises and disturbances irrelevant to environmental features, the extraneous data in one frame of 420kByte can be reduced to less than 4.2kByte by a binarization and filtering process.

Target recognition is executed by applying a recognition algorithm to these reduced 4.2 kByte data.

2.2.2 Preliminary test for the adjustment of SPMRS

The sensitivity of the ultrasonic range unit, the stepping motor resolution, the sampling period, the optimal number of sampling and the threshold value of the binarization were determined through preliminary experiments.

If there is deviation of the multiple reflection patterns for each reflector at the same test condition, SPMRS can not be operated correctly as a range sensor.

Mis-selection of the threshold value of binarization may lead to a loss of the environment feature information in the multiple reflection patterns. The threshold value must be selected so that the valuable information of the indoor feature is retained in the form of multiple reflections. In this paper, we select 2715(BCD) as a threshold value for the binarization.

If the step angle resolution is too large, it is not possible to obtain a sophisticated azimuth to determine the target location. On the other hand, if the angle is too small, there are too many data and it requires too much time to process the multiple reflection data.

The step motor resolution is selected to 1° in this paper and the sampling period is determined to be 10μs, two times of the ultrasonic source frequency of 49.7 kHz, to prevent aliasing.

2.3 Pre filter algorithm for SPMRS

Multiple reflection patterns for a particular scanning step are shown in Fig.9 at threshold values. Each multiple reflection pattern has more than one TOF, which is caused by an initial transmission of 56 cycles of ultrasonic wave when the ranging unit is fired to generate the sonar [7]. Therefore, the data obtained by SPMRS must be filtered to obtain the first reflected TOF via the filtering process. The filtering process divides the scanned multiple reflection data into groups according to the reflector number, and each group is filtered to obtain the first reflected TOF, and then the output is combined to make one frame of multiple reflection data, which consists of only the first arriving TOF with the unnecessary multiple TOFs filtered out.

(a) threshold 2705. (b) threshold 2715.

Fig.9 Multiple reflection waveform after binarization.

Target features such as the target type, distance and azimuth are extracted by applying a recognition algorithm to these data.

3 SPMRS characteristic curve

We execute a series of experiments to obtain the sensor characteristic curves for each environmental feature (Fig.4, Fig.6), and Fig.10 shows the experimental results obtained with all targets located 100cm apart from the SPMRS. The patterns are similar to those shown in Fig.8.

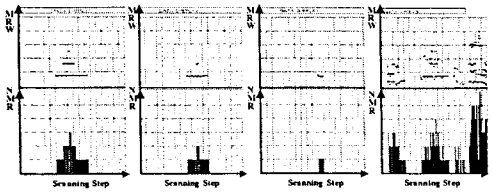

(a) (b) (c) (d)

Fig.10 Real multiple reflection patterns and number of multiple reflections for each target with the target 100cm apart from the reflector: (a) plane target with GMRS(1), (b) cylinder target with diameter 45cm with GMRS(1), (c)edge target with GMRS(3) and (d) corner target with GMRS(1).

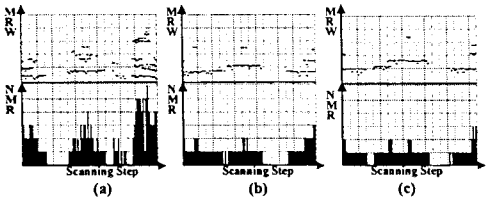

(a) (b) (c)

Fig.11 The multiple reflection patterns and number of multiple reflections according to the distance change between the reflector and the corner target: (a) at 100 cm, (b) at 150 cm, (c) at 200 cm.

We see three triangular GMRSs along the scanning direction for the corner target (Fig.8(d) and Fig.11), which is a feature peculiar to the corner target alone. The central GMRS of the corner target carries the distance and azimuth information between the reflector and corner target.

These preliminary experiments continued for each basic target at different locations to collect the preliminary data.

Fig.12 shows the experimental results and their error analyses.

True pos.		Measured Data		Absolute error		NMR	SD
Dist. (cm)	Azim (°)	Dist. (cm)	Azim (°)	Dist.Error (cm)	Azim.Error (°)	(turns)	(steps)
88	135	89	132	+1	−3	3	23
138	120	137	114	−1	−6	2	19
188	118	176	114	−12	−4	1	15
238	118	229	114	−9	−4	1	17

(a) plane target.

True pos.		Measured Data		Absolute error		NMR	SD
Dist. (cm)	Azim (°)	Dist. (cm)	Azim (°)	Dist.error (cm)	Azim.error (°)	(turns)	(steps)
88	125	95	127	+7	+2	4	32
138	125	130	131	+6	+6	3	28
188	125	191	129	+3	+4	2	26
238	125	241	129	+3	+4	2	26

(b) cylinder target.

True pos.		Measured Data		Absolute error		NMR	SD
Dist. (cm)	Azim (°)	Dist. (cm)	Azim (°)	Dist.error (cm)	Azim.error (°).	(turns)	(steps)
88	121	86	123	−2	+2	1	11
98	121	94	123	−4	+2	1	5
138	121	123	124	−15	+3	1	2
158	121	—	—	—	—	—	—

(c) edge target.

True pos.		Measured Data		Absolute error		NMR	SD
Dist. (cm)	Azim (°)	Dist. (cm)	Azim (°)	Dist.error (cm)	Azim.error (°)	(turns)	(steps)
138	135	137	135	−1	0	3	—
188	135	179	138	−9	+3	2	—
238	135	235	135	−3	−3	1	—

(d) corner target.

Fig.12 Recognition error analyses of feature such as a distance and azimuth for each target.

The characteristics of multiple reflection patterns for SPMRS based on these preliminary experimental results are:

(1) Multiple reflection patterns from a cylinder target are similar to the plane target but SD and NMR of cylinder target are shorter than that of the plane.

(2) The number of GMRS is more than three in the corner target, the distance and azimuth to the corner target satisfies the geometrical relation

$$X^2 + Y^2 = \rho^2 \ , \theta = \cos^{-1}\left(\frac{X}{Y}\right) \qquad (2)$$

and the target features such as the distance and azimuth are located at the central GMRS in case of the corner.

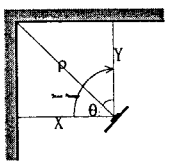

Fig.13 Geometrical configuration of two planes in a corner target.

(3) Multiple reflections do not occur in the edge target irrespective its distance from the reflector, and it has a rectangular GMRS.

We define the characteristic curves to discriminate target type as normalized inverse distance (NID) in Eq.(3).

$$NID = SD / D_T \ * NMR \qquad (3)$$

where **NID** is Normalized Inverse Distance (steps/cm*turns), **SD** and **NMR** are step distance (deg) and number of multiple reflections (turns), respectively, as defined in Fig.7, and $\mathbf{D_T}$ is distance to the target (cm).

The NID and NMR characteristic curves are calculated

using the data of Fig.12 and Eq.(3), except for the corner target which is calculated by Eq.(2).

Fig.13 shows a pair of NMR and NID as the characteristic curves of SPMRS, which is used in the recognition process.

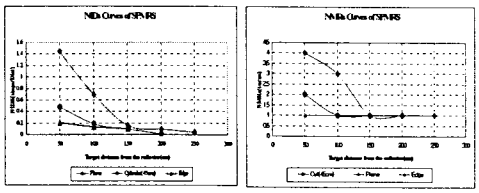

(a) NID plots. (b) NMR plots.

Fig.13 Characteristic curves of SPMRS range sensor.

4 Feature recognition algorithm and its application to the real indoor environment

4.1 Geometrical features of the SPMRS

The geometrical configuration of the SPMRS shown in Fig.14 is used to calculate features such as distance and azimuth to the target, where the rotation and translation matrices are defined in Eq.(4).

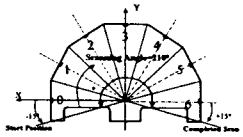

Fig.14. SPMRS coordinates.

The scan angle θ is increased in a clockwise direction from –15° to 195°, a total of 210°.

$$T^{c,i} = \begin{pmatrix} \cos\theta_i & -\sin\theta_i & 0 \\ \sin\theta_i & \cos\theta_i & 0 \\ 0 & 0 & 1 \end{pmatrix} \cdot T(t_x, t_y, 1) = \begin{bmatrix} 1 & 0 & t_x \\ 0 & 1 & t_y \\ 0 & 0 & 1 \end{bmatrix} \quad (4)$$

where r is the radius of the SPMRS, θ_i : rotated angle, t_x, t_y : ultrasonic sensor location from the rotation center of SPMRS.

The geometrical dimension is summarized in Table 1.

Table 1: Geometrical dimensions of the SPMRS

Symbol	Description	Dimension
R	Radius	37.5 (cm)
θ_i	Rotated Step angle	Calculated at maximum reflection step (°)
t_x, t_y	Translation	Calculated at maximum reflection step (cm)

4.2 Recognition algorithm and real environment test

We explain the recognition algorithm by pseudo code as shown in Algorithm 1.

Algorithm 1: SPMRS recognition algorithm

% Scanning and data gathering phase
Scan to get one frame of multiple reflection data (OFMRD)
Filter the OFMRD and group it into GMRSs
% Feature Extraction phase
For each GMRS
  Calculate SD, NMR, Td, Azimuth axis
  Calculate NID
  Find the target type by a pair of NID and NMR graph
  Find the azimuth angle and Distance to the target
End
% Refining Phase
For each detected target
  Change the edge, the plane and the cylinder in vicinity of the corner satisfying the following equation

$$X^2 + Y^2 = \rho^2 \quad ,\theta = \cos^{-1}\left(\frac{X}{Y}\right)$$

  into a corner target.
End

Fig.15(a) shows a pair of multiple reflection waveform and the number of multiple reflection obtained by the SPMRS, and the processed results are listed in Fig.15(b). Fig.15(c) shows the recognition procedure following Algorithm 1.

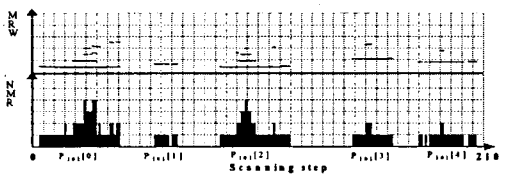

(a) MRW and NMR.

$P_{101}[k]$	Azim (°)	Dist (cm)	NIDs	NMRs	SDs	Detected Target Type	Error Azim (°)	Error Dist. (cm)
$P_{101}[0]$	15	99	2.45	4	38	Plane	–5	–1
$P_{101}[1]$	45	138	0.126	1	11	Corner	10	–1
$P_{101}[2]$	87	98	2.19	4	33	Plane	3	2
$P_{101}[3]$	144	177	0.273	2	19	Corner	–1	0
$P_{101}[4]$	179	146	0.499	2	27	Plane	1	2

(b) detected features and errors.

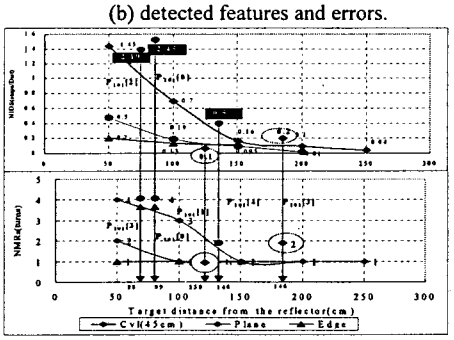

(c) recognition procedure.

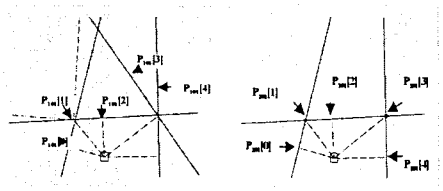

(d) before refining. (e) after refining.

Fig.15 Recognition result and error analysis at pos[101]: ■ indicates the recognized target correctly, and ○ indicates the recognized target incorrectly in (c).

In the first recognition phase, $P_{101}[1]$ and $P_{101}[3]$ are recognized incorrectly as edge and plane targets (Fig.15(d)), respectively, but all these features are corrected to corner targets by refining the process and considering the geometrical relationship between adjacent features (Fig.15(e)).

By continuing this data acquisition and recognition process while moving the SPMRS from Pos[102] to Pos[114], we can obtain recognition results as in Fig.16(a), where the recognized results overlap the real map for easy comparison of the true value with the recognized value.

Fig.16(b) shows the root mean square (RMS) error analysis result for the distance and azimuth at each location by Eq.(5).

$$DIST_{rms}[p]=\sqrt{\frac{\sum_{i=0}^{K}\left(DIST_R[i]-DIST_D[i]\right)^2}{K+1}},\quad AZIM_{rms}[p]=\sqrt{\frac{\sum_{i=0}^{K}\left(AZIM_R[i]-AZIM_D[i]\right)^2}{K+1}} \tag{5}$$

where p is location number in the test environment, ranging from 101 to 114, and K is a detected number of GMRSs at Pos[p], where the $DIST_R$,$DIST_D$ (or $AZIM_R$,$AZIM_D$) denote the true and the detected distance (or azimuth) data, respectively.

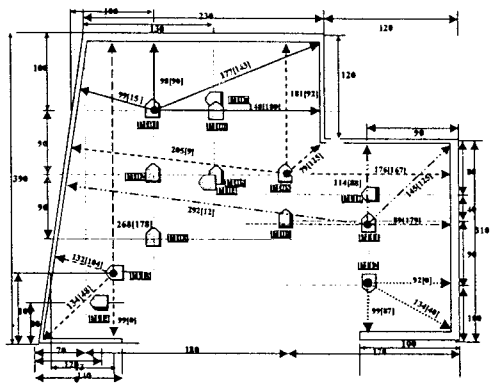

(a)

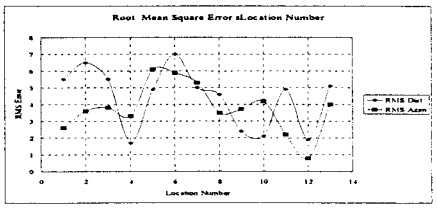

(b)

Fig.16. Environment modeling results by SPMRS: (a) recognized environment model,(b)RMS error analyses at each local position

In Fig.18(a), the P108 indicates a location number and the first number before and the second number inside of the brace indicate measured distance and measured azimuth angle, for example as 99[15] at P101 of Fig.17(a), respectively.

5 Conclusion

This paper proposes a new ultrasonic range sensor using multiple reflection properties of sonar, and a pair of sensor characteristic curves such as NIDs and NMRs obtained by the preliminary experiment.

Applying the proposed recognition algorithm to the test environment, we can obtained 4.3 cm of RMS distance error and 3.7° of RMS azimuth error, and three failures in target type recognition, respectively.

References

[1] B.Barshan, and R.KUC, Differentiating Sonar reflections from corners and plane by employing an intelligent Sensor, PAMI, Vol.12, No.6, pp560-569, June.1990.

[2] J.J.Hugh and F.Durrant-Whyte, Mobile robot Localization by Tracking Geometric Beacons, IEEE Trans. On Robotics and Automation, Vol.7.No.3. pp376-382, June.1991.

[3] D.Lee, The map-building and exploration strategies of a simple sonar-equipped robot, Cambridge Press, 1996,p59.

[4] R.Kuc and M.W.Siegel, Physically based simulation model for acoustic sensor for robot navigation, IEEE Trans. on PAMI9, No.6,pp776-777.Nov.1987.

[5] Roman Kuc, A spatial sampling criterion for sonar obstacle detection,IEEE Transaction on PAMI. Vol.12.No 7,pp 686-690,July 1990

[6] B.Bashan, B.Ayrulu, and S.W.Utete, Neural Network based Target Differentiation Using Sonar for Robotics Applications, IEEE Trans.R&A Vol.16.No.4, Aug.2000.

[7] Polaroid Corporation Technical Assistance, Ultrasonic Ranging System, 1992.